RAPID COMMUNICATIONS

PHYSICAL REVIEW B VOLUME 51, NUMBER 18 1 MAY 1995-II

Unrestricted Hartree-Fock study of transition-metal oxides: Spin and orbital ordering in perovskite-type lattice

T. Mizokawa and A. Fujimori
Department of Physics, University of Tokyo, Bunkyo-ku, Tokyo 113, Japan
(Received 9 January 1995)

We have performed spin- and orbital-unrestricted Hartree-Fock calculations on a realistic perovskite-type lattice model using electronic-structure parameters deduced from photoemission spectroscopy. For high-spin d^4 $LaMnO_3$, alternating $(3x^2-r^2)/(3y^2-r^2)$ orbital ordering is stabilized by Jahn-Teller distortion whereas for low-spin d^7 $RNiO_3$ (R is a rare earth), such a stabilization is suppressed by t_{2g}-e_g mixing caused by off-diagonal Coulomb terms. We have also studied the effect of $GdFeO_3$-type lattice distortion on the magnetic structures and the band gaps of $RNiO_3$ and $RTiO_3$.

$3d$ transition-metal oxides, in particular perovskite-type oxides, exhibit a variety of magnetic and electrical properties. For example, the physical properties of $RTiO_3$ (R is a rare earth), which belong to the Mott-Hubbard regime of the Zaanen-Sawatzky-Allen (ZSA) diagram,[1] have been studied as functions of the size of the R ion, i.e., as functions of the $GdFeO_3$-type lattice distortion, in which the TiO_6 octahedra forming the perovskite lattice are rotated as shown in Fig. 1(a).[2] The metallic phase of the doped Mott-Hubbard insulator $La_{1-x}Sr_xTiO_3$ behaves as a typical Fermi liquid.[3] On the other hand, metal-insulator transitions in the charge-transfer regime of the ZSA diagram have been investigated in $RNiO_3$ with various R ions.[4,5] The ferromagnetic (FM) metal $La_{1-x}Sr_xMnO_3$ can be regarded as a hole-doped antiferromagnetic (AFM) insulator $LaMnO_3$ and has attracted revived interest.[6]

In order to study the basic electronic structure of the $3d$ transition-metal oxides, their photoemission spectra have been analyzed using the cluster model or Anderson-impurity model,[1,7] where electron correlation related to a single transition-metal ion is exactly treated but the translational symmetry of the crystal lattice is ignored. In order to fundamentally understand their electronic properties, especially the effect of lattice distortion as well as that of spin and orbital ordering on their metal-insulator transitions, it is important to explicitly consider the translational symmetry. Since it is impossible to obtain the exact solutions of lattice models in the presence of strong electron-electron interaction, one has to employ certain approximations. The Hartree-Fock (HF) approximation is one of the most straightforward and well-defined approximations: In the case of integer band filling, it correctly gives the d bands which are split into upper and lower Hubbard bands for strong electron-electron interaction. Previously, orbital polarizations in degenerate Hubbard models have been studied by using the unrestricted HF approximation,[8] which has been generally discussed by Brandow.[9] Recently, models of the CuO_2 plane have been studied using the same approximation.[10,11]

In this paper, we report on the results of spin- an orbital-unrestricted HF calculations on a realistic perovskite-type lattice model using parameters deduced from the cluster-model analyses of photoemission spectra. The aim of the present study is twofold. First, we attempt to explain the various physical properties of $3d$ transition-metal oxides within the HF approximation. Second, we explore the limitation of the HF approximation and the necessity to consider electron correlation effects to understand their electronic properties.

We have employed the multiband d-p model (Anderson-lattice model) where we have included the full degeneracies of the transition-metal $3d$ orbitals and the oxygen $2p$ orbitals as well as on-site Coulomb and exchange interaction:

$$H=H_d+\varepsilon_p\sum_{\mathbf{k},l,\sigma}p^\dagger_{\mathbf{k},l\sigma}p_{\mathbf{k},l\sigma}+\sum_{\mathbf{k},l>l',\sigma}V^{pp}_{\mathbf{k},ll'}p^\dagger_{\mathbf{k},l\sigma}p_{\mathbf{k},l'\sigma}+\text{H.c.}+\sum_{\mathbf{k},l,\beta m,\sigma}V^{pd}_{\mathbf{k},l\beta m}p^\dagger_{\mathbf{k},l\sigma}d_{\mathbf{k},\beta m\sigma}+\text{H.c.},$$

$$H_d=\varepsilon^0_d\sum_{\alpha,\beta,m,\sigma}d^\dagger_{\alpha,\beta m\sigma}d_{\alpha,\beta m\sigma}+\sum_{\alpha,\beta,m,m',\sigma,\sigma'}h_{m\sigma,m'\sigma'}d^\dagger_{\alpha,\beta m\sigma}d_{\alpha,\beta m'\sigma'}+\sum_{\alpha,\beta,m}ud^\dagger_{\alpha,\beta m\uparrow}d_{\alpha,\beta m\uparrow}d^\dagger_{\alpha,\beta m\downarrow}d_{\alpha,\beta m\downarrow}$$

$$+\sum_{\alpha,\beta,m\neq m'}u'd^\dagger_{\alpha,\beta m\uparrow}d_{\alpha,\beta m\uparrow}d^\dagger_{\alpha,\beta m'\downarrow}d_{\alpha,\beta m'\downarrow}+\sum_{\alpha,\beta,m>m',\sigma}(u'-j)d^\dagger_{\alpha,\beta m\sigma}d_{\alpha,\beta m\sigma}d^\dagger_{\alpha,\beta m'\sigma}d_{\alpha,\beta m'\sigma}$$

$$+\sum_{\alpha,\beta,m\neq m'}j'd^\dagger_{\alpha,\beta m\uparrow}d_{\alpha,\beta m'\uparrow}d^\dagger_{\alpha,\beta m\downarrow}d_{\alpha,\beta m'\downarrow}+\sum_{\alpha,\beta,m\neq m'}jd^\dagger_{\alpha,\beta m\uparrow}d_{\alpha,\beta m'\uparrow}d^\dagger_{\alpha,\beta m'\downarrow}d_{\alpha,\beta m\downarrow},\qquad(1)$$

0163-1829/95/51(18)/12880(4)/$06.00

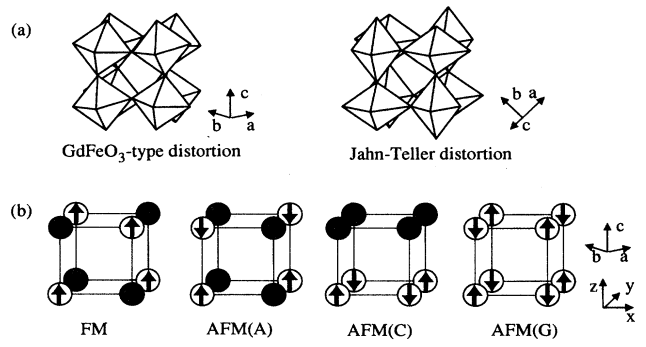

FIG. 1. (a) $GdFeO_3$-type distortion of the perovskite-type lattice (left) and the Jahn-Teller distortion of $LaMnO_3$ (right). (b) Typical spin- and orbital-ordered structures for the perovskites. Arrows indicate the spin polarization. Open and shaded circles represent different orbitals.

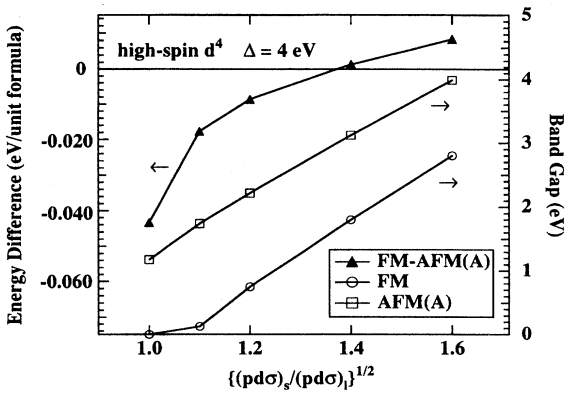

FIG. 2. Energy difference between the A-type AFM solution and the FM solution for the high-spin d^4 perovskite $LaMnO_3$ and the band gaps for the two solutions as functions of the degree of the Jahn-Teller distortion represented by the ratio $(pd\sigma)_s/(pd\sigma)_l$.

where $d^\dagger_{\mathbf{k},\beta m\sigma}\equiv(1/\sqrt{N})\Sigma_\alpha e^{i\mathbf{k}\cdot\mathbf{R}_\alpha}d^\dagger_{\alpha,\beta m\sigma}$ and $p^\dagger_{\mathbf{k},l\sigma}$ are Bloch electrons consisting of the transition-metal $3d$ and oxygen $2p$ orbitals, respectively. α and $\mathbf{k}$ label the unit cell and the wave vector in the first Brillouin zone. β and m run on the transition-metal atoms in the unit cell and the $3d$ orbitals on the transition-metal atom, respectively. l denotes the $2p$ orbitals in the unit cell. $V^{pp}_{\mathbf{k},ll'}$ and $V^{pd}_{\mathbf{k},lm}$ are nearest-neighbor p-p and p-d transfer integrals given in terms of Slater-Koster parameters $(pp\sigma)$, $(pp\pi)$, $(pd\sigma)$, and $(pd\pi)$.[12] $h_{m\sigma,m'\sigma'}$ represents crystal-field and spin-orbit interactions. The intra-atomic d-d interaction is expressed in terms of Kanamori parameters u, u', j, and j'.[13] In order to retain the rotational invariance of the d-d interaction term in real space, the off-diagonal j and j' terms should be included and the parameters should satisfy the relations $u'=u-2j$ and $j'=j$.[9,13,14] The mean-field Hamiltonian has ten order parameters of the form $\langle n^d_{\beta m\sigma}\rangle\equiv\langle d^\dagger_{\alpha,\beta m\sigma}d_{\alpha,\beta m\sigma}\rangle$ as coefficients for the diagonal $d^\dagger_{\mathbf{k},\beta m\sigma}d_{\mathbf{k},\beta m\sigma}$ terms and 45 order parameters of the form $\langle b^d_{\beta mm'\sigma\sigma'}\rangle\equiv\langle d^\dagger_{\alpha,\beta m\sigma}d_{\alpha,\beta m'\sigma'}\rangle$ for the off-diagonal $d^\dagger_{\mathbf{k},\beta m\sigma}d_{\mathbf{k},\beta m'\sigma'}$ $(m\neq m')$ terms per transition-metal ion, which are to be determined self-consistently.

The charge-transfer energy Δ for $d^n\rightarrow d^{n+1}\underline{L}$ is given by $\varepsilon^0_d-\varepsilon_p+nU$, where $U(=u-20/9j)$ is the multiplet average of the d-d Coulomb interaction. Kanamori parameters are related to Racah parameters A, B, and C through $u=A+4B+3C$ and $j=5/2B+C$. Values for Δ, U, and $(pd\sigma)$ have been obtained by the systematic cluster-model analyses of photoemission spectra for various transition-metal oxides.[1,7,14] Δ increases as the atomic number of the transition metal decreases and is estimated to be ~1 eV for $PrNiO_3$ (Ref. 15) and ~4 eV for $LaMnO_3$.[14,16] By extrapolation, we estimate $\Delta\sim7$ eV for $LaTiO_3$, which is similar to that obtained for Ti_2O_3.[17] U is estimated to be ~6–8 eV for late transition-metal oxides[1,14–16] and ~3–5 eV for early transition-metal oxides.[1,17] We have thus used the Δ, U, and $(pd\sigma)$ values listed in Table I. The ratio $(pd\sigma)/(pd\pi)$ is fixed at ~-2.16,[12,18] and $(pp\sigma)$ and $(pp\pi)$ at -0.60 and 0.15 eV, respectively.[18] B and C are fixed to free ion values or 80% of the atomic Hartree-Fock values.[19]

TABLE I. Parameters deduced from photoemission spectroscopy (in eV).

	Δ	U	j	$(pd\sigma)$
$RNiO_3$	1.0	7.0	0.88	−1.8
$RMnO_3$	4.0	5.5	0.76	−1.8
$RTiO_3$	7.0	4.0	0.64	−1.8

We iterated the self-consistency cycles of the HF calculation until all the order parameters converged to less than 2×10^{-4} by sampling 512 $\mathbf{k}$ points in the first Brillouin zone of the $GdFeO_3$ structure, whose unit cell contains four unit formulas. Here, the $GdFeO_3$ structure is obtained from the cubic perovskite structure by rotating the MO_6 octahedra (M is the transition metal) around the a axis. The $GdFeO_3$-type distortion reduces the M-O-M bond angle from 180°, thereby reducing the indirect overlap between neighboring d orbitals and hence the bandwidth. Basic magnetic structures for the perovskite-type oxides, namely, FM, A-type AFM, C-type AFM, and G-type AFM structure, are shown in Fig. 1(b) The figure also shows possible orbital ordering accompanying the magnetic ordering.

In high-spin d^4 and low-spin d^7 systems, where one of the e_g orbitals is occupied, there is an interesting interplay between spin and orbital ordering and Jahn-Teller distortion. The $Mn^{3+}(d^4)$ perovskite-type oxide $LaMnO_3$ is an insulator and shows A-type antiferromagnetism. Within the a-b plane, the e_g orbitals are polarized into alternating $3x^2-r^2$ and $3y^2-r^2$ orbitals accompanied by the Jahn-Teller distortion shown in Fig. 1(a).[6] Without the Jahn-Teller distortion, both the FM and A-type AFM solutions are accompanied by the $(3x^2-r^2)/(3y^2-r^2)$ orbital polarization with considerable mixture of $3z^2-r^2$; the total energy of the FM solution is lower because FM spin coupling is thus favored both within the a-b plane and between the a-b planes due to the orbital polarization. With the Jahn-Teller distortion, the orbital polarization becomes purely $(3x^2-r^2)/(3y^2-r^2)$ and the A-type AFM solution is strongly stabilized as shown in Fig. 2. Here, the magnitude of the Jahn-Teller distortion is represented by the ratio $(pd\sigma)_s/(pd\sigma)_l$, where $(pd\sigma)_s$ and $(pd\sigma)_l$ are transfer integrals for the shorter and longer Mn-O

bonds, respectively. This implies that, if one can somehow suppress the Jahn-Teller distortion, the system would turn from A-type AFM to FM. Indeed, the Jahn-Teller distortion is suppressed in $La_{1-x}Sr_xMnO_3$ by hole doping and the system becomes FM.[6] Figure 2 also shows that the band gap of the FM solution is smaller than that of the A-type AFM solution. This indicates that the metallization of $La_{1-x}Sr_xMnO_3$ is favored by the changes in the spin and the orbital polarization induced by hole doping.

Ni^{3+} (low-spin d^7) perovskite-type oxides, $PrNiO_3$ and $NdNiO_3$, show unusual magnetic structures, where each Ni ion is ferromagnetically coupled to three nearest neighbors and antiferromagnetically coupled to the other three.[5] In order to explain this magnetic structure, it has been proposed that the e_g orbitals are polarized into $3z^2-r^2$ and x^2-y^2 for the ferromagnetically coupled Ni pairs and are polarized into the same orbitals for the antiferromagnetically coupled Ni pairs.[5] Because the magnetic unit cell of $PrNiO_3$ is four times larger than that of the $GdFeO_3$-type structure, we could only study the simplified spin- and orbital-ordered structure shown in Fig. 1(b). The actual magnetic structure of $PrNiO_3$ can be viewed as a mixture of these four magnetic structures and hence calculations on these structures will give insight into the actual spin and orbital ordering. Here, we note that for $\Delta=1$ eV the high-spin AFM insulating state is the lowest and the low-spin FM metallic state is the second lowest, incompatible with experiment. This would be due to the lack of "Heitler-London-type" ($\uparrow\downarrow$-$\downarrow\uparrow$)-type electron correlation between a $3d$ electron and an oxygen $2p$ hole with antiparallel spins in the HF ground state. Indeed, in the cluster calculation, where electron correlation within the NiO_6 cluster is fully taken into account, the low-spin ^2E state is lower than the high-spin $^4T_1$ state for the same parameter set.[15] For larger $\Delta>\sim 2$ eV, the low-spin states exist as insulating metastable states in the HF band calculations. In order to study the changes in the magnitudes of the band gap for the various magnetic structures, therefore, we present below the results for $\Delta=2.4$ eV rather than $\Delta=1$ eV.

In the low-spin d^7 systems, the t_{2g} orbitals mix with the e_g orbitals though the off-diagonal Coulomb j' term. Therefore, Jahn-Teller distortion does not stabilize the A-type AFM solution significantly unlike the d^4 high-spin system. We denote the e_g orbitals which are mixed with t_{2g} orbitals as $3z^2-r^2$ and x^2-y^2. The FM and C-type AFM solutions, which have FM coupling along the c axis, favor the $(3z^2-r^2)/(x^2-y^2)$ orbital polarization, while the A-type AFM solution has $(3x^2-r^2)/(3y^2-r^2)$ orbital polarization. The total energies for the various solutions are plotted in Fig. 3 as functions of the Ni-O-Ni bond angle. The FM solution and the A-type AFM solution are very close in energy, suggesting that the complicated magnetic structure, where both the FM coupling and AFM coupling coexist and the FM coupling within the a-b plane and that between the a-b planes are competing, may be realized in these compounds. In Fig. 3, the band gaps for these solutions are also plotted as functions of the Ni-O-Ni bond angle. As the bond angle decreases from 160° to 150°, the band gaps increases by ~ 0.1 eV for any spin- and orbital-ordered structures. This explains the experimental observation that the metal-insulator transition temperature increases in going from $PrNiO_3$ ($\angle$Ni-O-Ni$\sim$157°) to $NdNiO_3$ ($\angle$Ni-O-Ni$\sim$156°).[3]

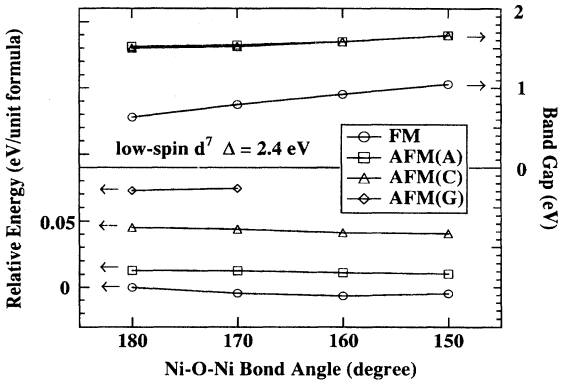

FIG. 3. Total energies and the band gaps for various spin- and orbital-ordered states for the low-spin d^7 perovskites $RNiO_3$ as functions of the Ni-O-Ni bond angle.

Finally, we have investigated the d^1 system $RTiO_3$, whose $GdFeO_3$-type distortion influences the relative stability of the AFM and FM states. $LaTiO_3$, where the $GdFeO_3$-type distortion is rather small, is an AFM insulator with a small band gap of ~ 0.1 eV.[2,20] In more distorted $YTiO_3$ and $GdTiO_3$, Ti-Ti spin coupling is found to be FM and the band gaps become as large as ~ 1 eV.[2,20] According to the HF calculations, the $GdFeO_3$-type distortion removes the threefold degeneracy of the t_{2g} band, and without spin-orbit interaction the FM where the yz and zx orbitals are alternatingly occupied is found to be the lowest. However, if we include spin-orbit interaction, the spin and orbital cannot be polarized independently. The combination of the spin-orbit interaction and the $GdFeO_3$-type distortion favors the occupancy of the $(zx+iyx)\uparrow$ or $(zx-iyx)\downarrow$ spin orbital. Then the G-type AFM solution where these two spin orbitals are alternatingly occupied or the FM solution where one of them is occupied is realized. The total energies of the FM and the G-type AFM solutions are compared in Fig. 4, where one can see that the FM solution becomes stable relative to the G-type AFM one as the distortion increases. This explains why the weakly distorted $LaTiO_3$ is AFM and the strongly distorted $YTiO_3$ is FM.

The $GdFeO_3$-type distortion also makes some e_g character hybridized into the t_{2g} band. Since the e_g character leads

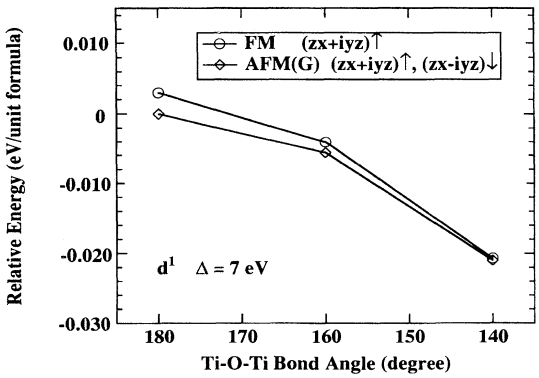

FIG. 4. Total energies of the FM and AFM solutions for the d^1 perovskites $RTiO_3$ as functions of the Ti-O-Ti bond angle.

to an increase in the bandwidth, the distortion does not necessarily reduce the bandwidth as expected from a simple model where only the t_{2g} orbitals are considered.[2] Indeed, the calculated band gap 2–3 eV for $R\mathrm{TiO_3}$ is hardly changed by the distortion both in the AFM and FM solutions in disagreement with the experimental results.[2] Uncertainties in the parameter values for the early transition-metal oxides exist but are not large enough to explain this disagreement. This may indicate the limitation of the HF approximation: The breakdown of Koopmans' theorem due to strong orbital relaxation and/or strong electron correlation (i.e., fluctuations around the HF ground state) will reduce the band gaps. Such a reduction would be stronger for the weakly distorted $\mathrm{LaTiO_3}$ than for the strongly distorted $\mathrm{YTiO_3}$ since the effective Coulomb interaction would be stronger for purer t_{2g} states, which are less strongly hybridized with oxygen $2p$ states, than for the t_{2g}-e_g mixed states. One can also conclude the reduction of the band gaps due to electron correlation would be stronger in Mott-Hubbard insulators, where the states near the Fermi level are dominated by the $3d$ character, than that in charge-transfer insulators, where the states near the Fermi level are strong mixtures of the $3d$ and oxygen $2p$ states.

In conclusion, the spin- and orbital-unrestricted HF calculations have revealed various types of spin and orbital ordering in the distorted perovskite-type $3d$ transition-metal oxides, thus explaining many experimental results. Some disagreement with experiment, on the other hand, shows the limitation of the HF approximation and the importance of electron correlation: In the Mott-Hubbard regime, the band gaps are overestimated because of the neglect of fluctuations around the HF ground state. In the charge-transfer regime with small Δ, the stability of the low-spin state is underestimated due to the lack of "Heitler-London-type" correlation. The unrestricted HF results thus provide us with well-defined mean-field states into which electron correlation effects are to be incorporated, enabling us to gain more insight into electron correlation in the $3d$ transition-metal oxides.

The authors wish to thank Dr. N. Hamada for valuable discussions. Calculations were performed on a VAX computer in Meson Science Laboratory, University of Tokyo. The present work is supported by a Grant-In-Aid for Scientific Research from the Ministry of Education, Science and Culture, Japan,

[1] J. Zaanen, G. A. Sawatzky, and J. W. Allen, Phys. Rev. Lett. **55**, 418 (1985); S. Hüfner, Z. Phys. B **61**, 135 (1985).

[2] D. A. Crandles, T. Timusk, J. D. Garrett, and J. E. Greedan, Physica C **201**, 407 (1992).

[3] T. Fujishima, Y. Tokura, T. Arima, and S. Uchida, Phys. Rev. B **46**, 11 167 (1992); Y. Tokura, Y. Taguchi, Y. Okada, Y. Fujishima, T. Arima, K. Kumagai, and Y. Iye, Phys. Rev. Lett. **70**, 2126 (1993).

[4] J. B. Torrance, P. Lacorre, A. I. Nazzal, E. J. Ansaldo, and Ch. Niedermayer, Phys. Rev. B **45**, 8209 (1992).

[5] J. L. García-Muñoz, J. Rodríguez-Carvajal, and P. Lacorre, Europhys. Lett. **20**, 241 (1992); Phys. Rev. B **50**, 978 (1994).

[6] Y. Tokura, A. Urushibara, Y. Moritomo, T. Arima, A. Asamitsu, G. Kido, and N. Furukawa, J. Phys. Soc. Jpn. **63**, 3931 (1994).

[7] A. Fujimori and F. Minami, Phys. Rev. B **35**, 957 (1984).

[8] M. Cyrot and C. Lyon-Caen, J. Phys. (Paris) **36**, 253 (1975); J. Ashekenazi and M. Weger, Adv. Phys. **22**, 207 (1973); C. Castellani, C. R. Natoli, and J. Ranninger, Phys. Rev. B **18**, 4945 (1975).

[9] B. H. Brandow, Adv. Phys. **26**, 651 (1977).

[10] J. B. Grant and A. K. McMahan, Phys. Rev. Lett. **66**, 488 (1991); Phys. Rev. B **46**, 8440 (1992).

[11] S. Nimkar, D. D. Sarma, H. R. Krishnamurthy, and S. Ramasesha, Phys. Rev. B **48**, 7355 (1993).

[12] W. A. Harrison, *Electronic Structure and the Properties of Solids* (Dover, New York, 1989).

[13] J. Kanamori, Prog. Theor. Phys. **30**, 275 (1963).

[14] A. E. Bocquet, T. Mizokawa, T. Saitoh, H. Namatame, and A. Fujimori, Phys. Rev. B **46**, 3771 (1992).

[15] T. Mizokawa, A. Fujimori, T. Arima, Y. Tokura, and N. Mori (unpublished).

[16] T. Saitoh, A. E. Bocquet, T. Mizokawa, H. Namatame, A. Fujimori, M. Abbate, Y. Takeda, and M. Takano, Phys. Rev. B (to be published).

[17] T. Uozumi, K. Okada, and A. Kotani, J. Phys. Soc. Jpn. **62**, 2595 (1993).

[18] L. F. Mattheiss, Phys. Rev. B **5**, 290 (1972); **6**, 4718 (1972).

[19] F. M. F. de Groot, J. C. Fuggle, B. T. Tole, and G. A. Sawatzky, Phys. Rev. B **42**, 5459 (1990).

[20] J. P. Goral, J. E. Greedan, and D. A. MacLean, J. Solid State Chem. **43**, 244 (1982).